

# Jahn-Teller Effects in the Electron Paramagnetic Resonance of $\text{Cu}^{++}$ in $\text{Ca}(\text{OH})_2^\dagger$

R. G. WILSON,\* F. HOLUJ, AND N. E. HEDGECOCK

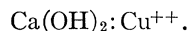
Department of Physics, University of Windsor, Windsor 11, Canada

(Received 20 June 1969)

The EPR spectra of  $\text{Cu}^{++}$  present as an impurity in hexagonal  $\text{Ca}(\text{OH})_2$  has been investigated in the temperature range 85–380°K. Below 145°K, the EPR spectra, I, show a “static” Jahn-Teller effect (JTE) with  $g_{11}=2.421$ ,  $g_{\perp}=2.079$ ,  $^{65}A=142\pm 1$  G,  $^{65}B=132\pm 1$  G,  $^{65}B=^{62}B=0\pm 3$  G. Above 145°K, the spectrum, III, is due to the “dynamic” JTE with  $g_{11}=2.241$ ,  $g_{\perp}=2.172$ ,  $A=48$  G and  $B=37$  G. These values for III are almost exact averages of the corresponding values for I when the latter executes hindered rotation about the hexagonal  $c$  axis. Further support for this interpretation is provided by the studies of peak-height dependence on temperature for both the static and dynamic spectra.

## I. INTRODUCTION

THIS paper deals with the static and dynamic Jahn-Teller effects (JTE) in the system



JTE has been observed in the EPR spectroscopy of a number of ions of the first transition series having a degenerate electron orbital ground state. The simplest is the state  ${}^2E_g$  (e.g.,  $\text{Sc}^{+2}$  in cubic symmetry or  $\text{Cu}^{+2}$  in octahedral symmetry).<sup>1</sup> JTE comes in a variety of manifestations: a “static” distortion leading to the lowering of the symmetry of the immediate environment; a “vibrational” distortion of the environment (“dynamic” JTE); and, recently, a third form, “tunneling” JTE was observed in  $\text{MgO}:\text{Cu}^{++}$ ,  $\text{CaO}:\text{Cu}^{++}$ ,  $\text{CaF}_2:\text{Sc}^{++}$ , and  $\text{SrF}_2:\text{Sc}^{++}$  systems.<sup>2–4</sup> JTE has received an extensive theoretical treatment.<sup>5–10</sup>

## II. $\text{Ca}(\text{OH})_2$ CRYSTALS AND EXPERIMENTAL

X-ray studies have shown<sup>11–15</sup>  $\text{Ca}(\text{OH})_2$  to belong to the hexagonal system, with space group  $P(3,2/m,1)$

( $\text{CdI}_2$  type or  $D_{3d}^8$ ). The Ca atoms lie in the invariant positions (0,0,0), with point symmetry  $L_{3d}$ . The oxygen and hydrogen atoms lie in the special positions  $\pm(\frac{1}{3}, \frac{2}{3}, z_0)$  and  $\pm(\frac{1}{3}, \frac{2}{3}, z_h)$ , respectively, both with point symmetry  $3m$ . The hydrogen positions were first postulated by Bernal and Megaw.<sup>12</sup> They have since been confirmed by x-ray diffraction,<sup>13,14</sup> neutron diffraction,<sup>15</sup> and nuclear magnetic resonance.<sup>16</sup>

The  $\text{Ca}(\text{OH})_2$  structure consists of layers of two sheets of hydroxyls parallel to the basal plane (0001), with a sheet of Ca atoms between them. Figure 1 shows that each Ca atom lies between six OH groups forming an octahedron which is slightly compressed along the  $c$  axis. Weak van der Waals forces bind the opposed hydroxyl sheets. Neutron diffraction studies revealed that thermal motion of hydrogen is confined mainly to hydrogen layers normal to the  $c$  axis. Consequently, there are no hydrogen bonds. The observed softness (2 on the Mohs' scale) and a perfect cleavage in the basal plane also confirm this.

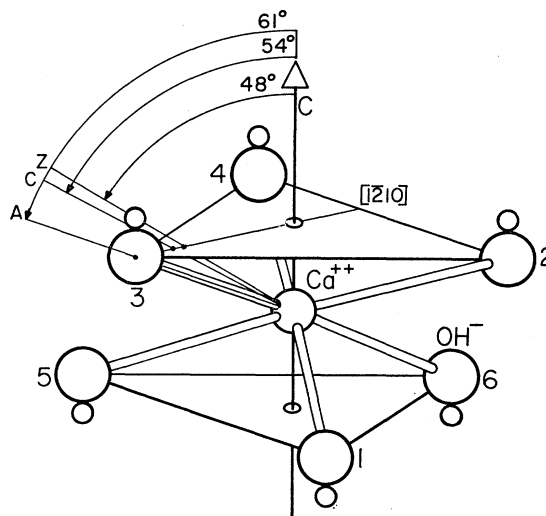


FIG. 1. Geometry of  $\text{Cu}^{++}$  site in  $\text{Ca}(\text{OH})_2$ . The octahedron is slightly compressed. The angle  $\gamma$  for undistorted octahedron is  $54^\circ$  (line C). The line  $z$  refers to the  $z$  axis of the static spectrum I.

<sup>†</sup> Work supported by National Research Council of Canada.

\* Holder of a National Research Council of Canada Scholarship.

<sup>1</sup> All the older and recent references of JTE will be found in M. D. Sturge, in *Solid State Physics*, edited by F. Seitz, D. Turnbull, and H. Ehrenreich (Academic, New York, 1967) Vol. 20, p. 91.

<sup>2</sup> R. E. Coffman, *Phys. Letters* **13**, 475 (1955); **21**, 381 (1966); *J. Chem. Phys.* **48**, 609 (1968).

<sup>3</sup> R. E. Coffman, D. L. Lyle, and D. R. Mattison, *J. Phys. Chem.* **72**, 1392 (1968).

<sup>4</sup> U. T. Höchli, *Phys. Rev.* **162**, 262 (1967).

<sup>5</sup> J. H. van Vleck, *J. Chem. Phys.* **1**, 72 (1939).

<sup>6</sup> B. Bleaney, K. D. Bowers, and M. H. L. Pryce, *Proc. Roy. Soc. (London)* **A228**, 166 (1954).

<sup>7</sup> U. Öpik and M. H. L. Pryce, *Proc. Roy. Soc. (London)* **A238**, 425 (1957).

<sup>8</sup> M. C. M. O'Brien, *Proc. Roy. Soc. (London)* **A281**, 323 (1964).

<sup>9</sup> I. B. Bersuker, *Zh. Eksperim. i Teor. Fiz.* **43**, 1315 (1962) [*Soviet Phys. JETP* **16**, 933 (1963)]; I. B. Bersuker, S. S. Budnikov, B. G. Vekhter, and B. I. Chinik, *Fiz. Tverd. Tela* **6**, 2583 (1964) [*Soviet Phys. Solid State* **6**, 2059 (1965)].

<sup>10</sup> F. S. Ham, *Phys. Rev.* **166**, 307 (1968).

<sup>11</sup> H. D. Megaw, *Proc. Roy. Soc. (London)* **A142**, 198 (1933).

<sup>12</sup> J. D. Bernal and H. D. Megaw, *Proc. Roy. Soc. (London)* **A151**, 384 (1935).

<sup>13</sup> H. E. Petch, *Can. J. Phys.* **35**, 983 (1957).

<sup>14</sup> H. E. Petch, *Acta Cryst.* **14**, 950 (1961).

<sup>15</sup> W. R. Busing and H. A. Levy, *J. Chem. Phys.* **26**, 563 (1957).

<sup>16</sup> D. M. Henderson and H. S. Gutowsky, *Am. Mineral.* **47**, 1231 (1962).

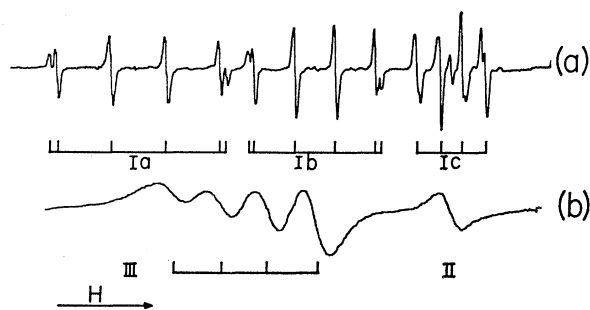


FIG. 2. (a) A general orientation of  $\mathbf{H}$ , illustrating the three complexes of spectrum I at  $87^\circ\text{K}$ . Note that Ia shows superhyperfine splitting. (b) Spectrum III at a general orientation of  $\mathbf{H}$ , at RT. Illustration of a case for which  $T_2$  depends on  $m_l$ .

Single crystals of  $\text{Ca}(\text{OH})_2$  were obtained by slow diffusion of  $\text{NaOH}$  and  $\text{CaCl}_2$  in a solution free of  $\text{CO}_2$ . They were doped with  $\text{Cu}^{++}$  during their growth in the solution.

An X-band spectrometer, utilizing a circulator, and a K-band spectrometer using a simple detection method, were used. The PSD operated at 100 kc/sec. A crystal-rotating mechanism developed earlier in this laboratory was employed for anisotropy studies.<sup>17</sup> This mechanism enabled the crystal to be rotated about a horizontal axis. Using this device, and rotating the magnet about its vertical axis, any arbitrary orientation of the crystal relative to the external magnetic field could be attained. Cavities for liquid-nitrogen to room-temperature work were of glass, with inner surface sputtered with gold. All cavities had loaded  $Q$ 's in the range 3000–6000 and operated in the cylindrical  $\text{TE}_{011}$  mode. Temperatures

were measured with uncalibrated thermocouples of Cu-constantan.

### III. EPR SPECTRUM AT $87^\circ\text{K}$

#### A. General Remarks

The EPR spectrum is due to three main Cu complexes, which are easily identified by their characteristic four-line hyperfine structure (hfs) lines. All three complexes are visible in Fig. 2(a). Incidentally, this spectrum also shows a superhyperfine structure consisting of a variable number of subcomponents. Five of them have been definitely counted. If these were due to the hydrogen of six neighboring OH groups, then a maximum of seven should be visible. Figure 3(a) shows the same spectrum when  $\mathbf{H}$  was along the  $c$  axis. We shall call it spectrum I or  $I_a$ , etc. Flanking I is another spectrum—we shall call it spectrum II—which in many respects is similar to I; it is most clearly visible in Fig. 3(d). It differs from I in two important respects: (a) It persists almost unchanged right up to room temperature (RT). (b) The magnetic axes are oriented slightly differently (the difference is about  $1^\circ$ ) from those of I. In view of this [especially point (a)], II can be interpreted as originating from a  $\text{Cu}^{++}$  situated in the  $\text{Ca}^{++}$  site distorted by electrostatic rather than JTE forces.

#### B. Characteristics of Spectrum I

Spectrum I is axial. Figure 1 shows that the axis (line  $Z$ ) is tilted  $48^\circ$  from the  $c$  axis in the  $(1\bar{2}10)$

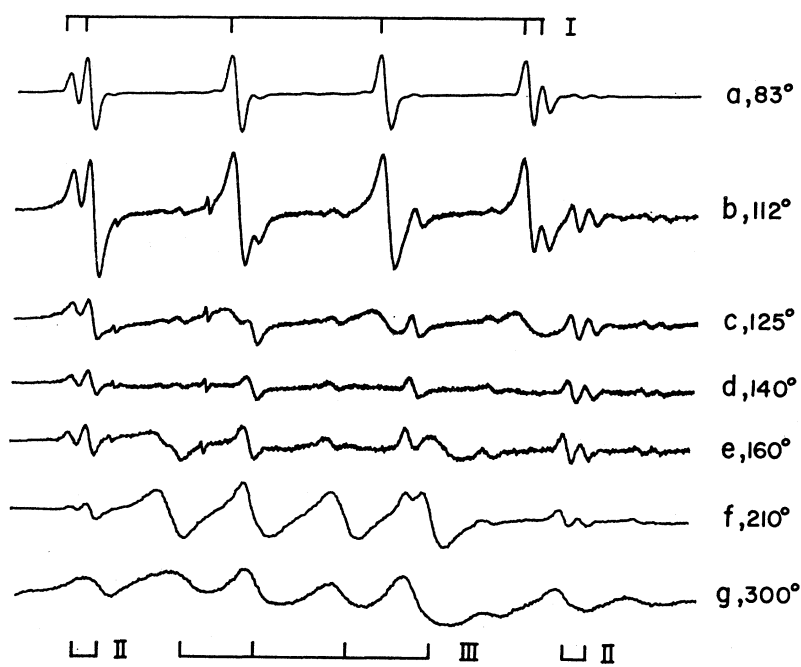


FIG. 3. Temperature dependence of the EPR spectra at K band for the case when  $\mathbf{H} \parallel c$ . The temperature in  $^\circ\text{K}$  is shown beside each trace. (d) shows a transition temperature at which only spectrum II is clearly visible.

<sup>17</sup> F. Holuj, Can. J. Phys. 46, 287 (1968).

TABLE I. Spin-Hamiltonian parameters of  $\text{Cu}^{++}$  in  $\text{Ca}(\text{OH})_2$ . II refers to room temperature.

Spectrum	$g_{11}$	$g_{\perp}$	$^{65}\text{A}$ (G)	$^{63}\text{A}$ (G)	$\kappa$	$A/P$	$w$	$u$
I (87°K)	$2.421 \pm 0.001$	$2.079 \pm 0.001$	$142 \pm 1$	$132 \pm 1$	0.357	-0.460	0.0543	0.0442
II	$2.401 \pm 0.001$	2.081	$151 \pm 1$	$140 \pm 1$	0.358	-0.485	0.0517	0.0447

plane. This direction, significantly enough, coincides with the plane formed by the hydroxyls 1-2-4-5. Figure 4 shows the angular variations of I in the  $(1\bar{2}10)$  plane.

The spectrum was analyzed using the axial spin Hamiltonian for  $S=\frac{1}{2}$  and  $I=\frac{3}{2}$  and  $\Delta M=\pm 1$  and  $\Delta m=0$ :

$$\mathcal{H} = g\beta_{11}S_zH_z + \beta g_{\perp}(S_xH_x + S_yH_y) + AS_zI_z + B(S_xI_x + S_yI_y).$$

Quadrupolar and nuclear Zeeman terms have been neglected. The expected resonances are<sup>18</sup>

$$H = g\beta H_0 + Km + \frac{B^2(A^2 + K^2)}{4g\beta H_0 K^2} (15/4 - m^2). \quad (1)$$

With an angle  $\theta$  between the magnetic field  $H_0$  and the  $z$ -principal axis of the  $g$  tensor,  $g$  and  $K$  are defined by  $g^2 = g_{11}^2 \cos^2\theta + g_{\perp}^2 \sin^2\theta$  and  $K^2 g_{\perp}^2 = A^2 g_{11}^2 \cos^2\theta + B^2 g_{\perp}^2$

$\times \sin^2\theta$ . Table I summarizes the result of the analysis of the spectrum on the basis of Eq. (1). It can be seen from the curves referring to I in Fig. 4 that the parameter  $B$  is very small. It is less than the linewidth of 10 G.

The remaining parameters of I in Table I have been obtained using the expressions<sup>6</sup>

$$g_{11} = g_0 + 8w - 3u^2 - 4uw, \quad (2)$$

$$g_{\perp} = g_0 + 2u - 4w^2, \quad (3)$$

$$A/P = -\kappa(1-u^2) - 4/7 + (6/7)u + 8w - (3/7)u^2 - (40/7)uw \dots, \quad (4)$$

$$B/P = -\kappa(1-1/2u^2-2w^2) + 2/7 + (11/7)u + (9/14)u^2 - (4/7)w^2 \dots, \quad (5)$$

where  $g_0 = 2.0023$ ,  $P = g_0\beta\gamma\beta_N\langle r^{-3} \rangle \approx 0.036 \text{ cm}^{-1}$  (for free  $\text{Cu}^{++}$  ion), and  $\kappa$  is the contact term (0.36 for free  $\text{Cu}^{++}$  ion).<sup>19</sup>  $w$  and  $u$  are the spin-orbit interaction constants

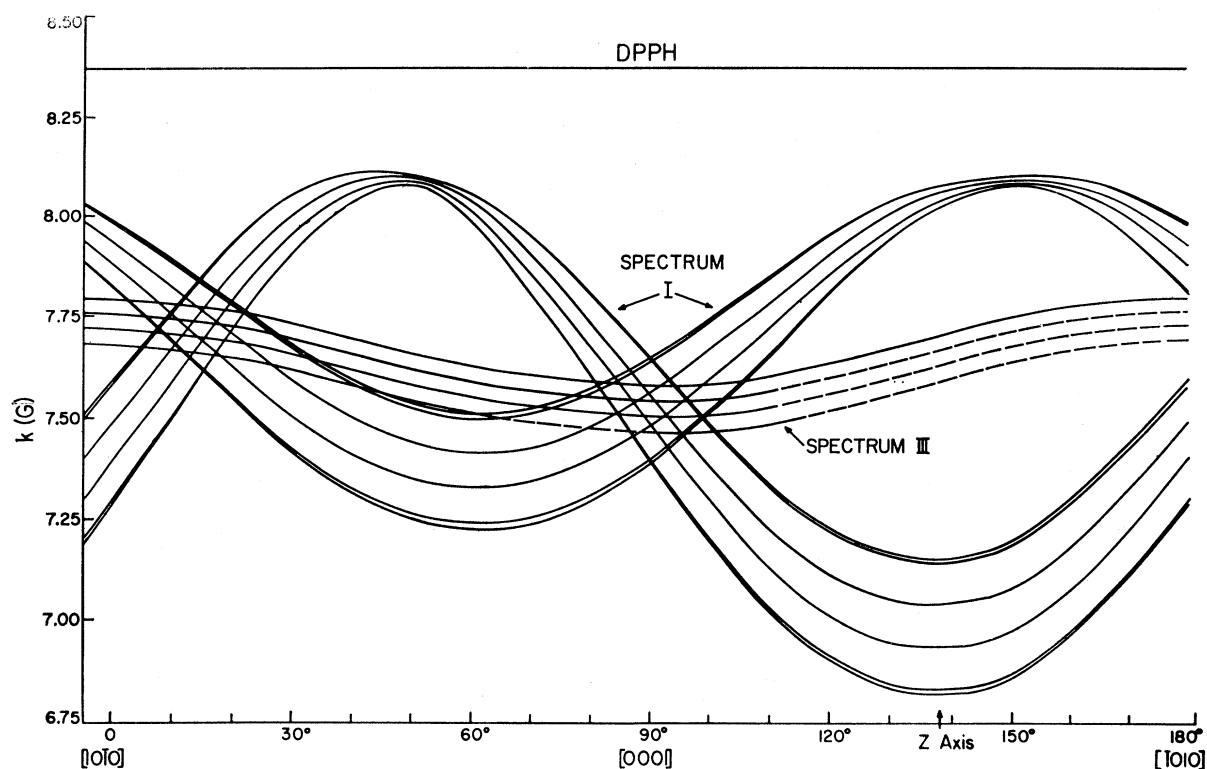


FIG. 4. Angular variation of the EPR spectra of  $\text{Ca}(\text{OH})_2:\text{Cu}^{++}$  in the  $(1\bar{2}10)$  plane. The curves for I and III were obtained at  $T=85$  and  $300^\circ\text{K}$ , respectively.

<sup>18</sup> W. Low, in *Solid State Physics*, edited by F. Seitz and D. Turnbull (Academic, New York, 1960), Suppl. 2.

<sup>19</sup> J. F. Gibson, D. J. E. Ingram, and D. Schonland, *Discussions Faraday Soc.* 26, 72 (1958).

TABLE II. Spin-Hamiltonian parameters of  $\text{Cu}^{++}$  in  $\text{Ca}(\text{OH})_2$ . High-temperature spectrum (III).

	Calculated		Experimental		
	Eq. (6)	Eq. (7)	K band 175°K	X band 300°K	X band 300°K
$g_{11}$	2.230	2.181	2.241	2.241	2.238
$g_{\perp}$	2.171	2.181	...	2.172	2.170
$A$	58		58	~48	48
$B$	32			~34	37

$-\lambda/E_1$  and  $-\lambda/E_2$ .  $E_1$  and  $E_2$  are the energies of the  ${}^2B_2$  and  ${}^2E$  excited terms of the  $3d$  hole above the  ${}^2B_1$  ground term of the tetragonally distorted octahedron.<sup>20</sup>

Table I also includes the spin-Hamiltonian parameters of spectrum II at RT. It has been inserted to stress the similarity of the two spectra. We have to make this remark about I. We looked very carefully for a possible anisotropy in I in the plane normal to the  $z$  axis, i.e., for any possible inequalities  $g_x \neq g_y \neq g_{\perp}$  or  $A_x \neq A_y \neq B$ , which might indicate the presence of the inversion splitting of the ground state.<sup>8,9</sup> To within the accuracy of the experiment, we found I perfectly axial in all respects. This agrees with the findings of Breen, Krupka, and Williams<sup>21</sup> in  $\text{Mg}_3\text{La}_2(\text{NO}_3)_{12} \cdot 24\text{H}_2\text{O}$  after they reexamined this system, which was originally studied by Bleaney, Bowers, and Trenam.<sup>22</sup>

#### IV. HIGH-TEMPERATURE SPECTRUM (III)

The sequence of events occurring between 87 and 300°K for the case when  $\mathbf{H}$  was along the  $c$  axis is shown in Figs. 3(a)–3(g). Figure 3(g) shows that at room temperature III, too, tends to broaden. As can be seen, III is best visible in the trace 3(f).

The angular variation of III is indicated in Fig. 4. A most significant fact emerges from these figures: The resonances of III are approximately the averages of those of I. For this purpose, if we express the  $g$  tensors of the three complexes I in a coordinate system whose  $z$  axis is parallel to the  $c$  axis we get, on averaging,

$$\begin{aligned} g_{11}' &= g_{11} \cos^2\alpha + g_{\perp} \sin^2\alpha, \\ g_{\perp}' &= \frac{1}{2}(g_{11} \sin^2\alpha + g_{\perp} \cos^2\alpha + g_{\perp}), \end{aligned} \quad (6)$$

where the unprimed quantities refer to spectrum I and  $\alpha$  is 48° (see Fig. 1). Analogous equations hold also for  $A'$  and  $B'$ .

The results of analysis of III are presented in Table II. Calculated and experimental quantities are close enough to confirm Eqs. (6).

Now, if the averaging occurred because of transitions to the excited levels, the resulting  $g$  factor would depend

on which inversion level was involved. For example, if this level were  $A_{1g}$ , then<sup>8</sup>

$$g'' = g_0 + 4u, \quad (7)$$

where  $u=w$  (approximately). This averaging would therefore lead to an isotropic  $g$  factor.

#### V. DISCUSSION OF THE RESULTS

When discussing the state  ${}^2E_g$ , it is customary to use a two-dimensional space formed from the octahedral normal coordinates  $Q_2$  and  $Q_3$  of the  $E_g$  nuclear vibrational mode.<sup>5</sup> Bersuker<sup>9</sup> and Sturge<sup>1</sup> used the following coordinates:

$$Q_2^{(i)} = \rho \sin(\theta - \Phi_i), \quad Q_3^{(i)} = \rho \cos(\theta - \Phi_i), \quad (8)$$

where  $(i) = 1, 2, 3$  refers to the three tetragonal distortions of the octahedron by displacing the ions located on the  $z$ ,  $x$  and  $y$  axes, respectively. Here,  $\Phi_1 = 0^\circ$ ,  $\Phi_2 = +120^\circ$ , and  $\Phi_3 = -120^\circ$ .  $Q_2^{(1)}$  transforms as  $(x^2 - y^2)$  and  $Q_3^{(1)}$  as  $(3z^2 - r^2)$ , etc. The  $\text{Cu}(\text{OH})_4^{2-}$  cluster vibrations important in JTE are those involving the  $\theta$  coordinates with the potential-energy minimum coinciding with  $(\theta - \Phi_i) = 0$  and  $\rho = \text{const.}$ <sup>23</sup> The vibrations in  $\rho$  are taken to be those of the undistorted octahedron.

O'Brien<sup>8</sup> visualizes the origin of III as follows. If one plots the dependence of electronic potential for  $\rho = \text{const}$  as a function of  $\theta$ , one obtains, for the ground state, a "warped" surface with minima at  $(\theta - \Phi_i) = 0$ . The three tetragonal deformations for which  $i = 1, 2, 3$  have equal energies. In this presentation, therefore, the spectrum I originates from the nearly threefold degenerate ground vibrational state  $G$ . It is degenerate because of lack of vibrational interaction between the subcomponents. As Ham<sup>10</sup> and Höchli<sup>4</sup> point out, one deformation may be favored as a result of strain, etc. But on a macroscopic scale even this may average out.

In contrast, the excited states  $E_g$ ,  $A_{1g}$  will be split by this mutual interaction. Irrespective of the source of this interaction,<sup>9</sup> the most important result is that if a state is originally in  $G$  at  $\theta = 0$  (say), then upon thermal excitation to higher levels, it may eventually relax back to  $G$ , but a different  $\theta$ . This mechanism was actually mentioned as a possible one by O'Brien.<sup>8</sup>

We visualize this mechanism causing the system to jump in a random fashion between the three inequivalent positions available to it at any orientation of  $\mathbf{H}$ .<sup>24</sup> The resulting averaging must follow Eq. (6). Alternatively, we can look on the system as undergoing hindered "rotation" about the  $c$  axis.

We studied carefully the temperature variation of spectra I and III. Figure 5 gives the graphs of logarithms of line peak heights,  $I_p$  versus  $T^{-1}$ . At  $X$ - and  $K$ -band frequencies  $\mathbf{H}$  was parallel or perpendicular to  $c$ . The three growth curves for spectrum III give activation

<sup>23</sup> Figure 7 of Ref. 1.

<sup>24</sup> A. Abragam, *The Principles of Nuclear Magnetism* (Oxford U. P., New York, 1961), pp. 447–451.

<sup>20</sup> J. S. Griffith, *The Theory of Transition-Metal Ions* (Cambridge U. P., New York, 1961), p. 343.

<sup>21</sup> D. P. Breen, D. C. Krupka, and F. I. B. Williams, *Phys. Rev.* **179**, 241 (1969).

<sup>22</sup> B. Bleaney, K. D. Bowers, and R. S. Trenam, *Proc. Roy. Soc. (London)* **A228**, 157 (1955).

energies of 1364, 959, and 1272  $\text{cm}^{-1}$ , respectively. An average, therefore, is  $\Delta_I = 1198 \pm 300 \text{ cm}^{-1}$ . The three decay curves of spectrum I yield 1669, 1113, and 1309  $\text{cm}^{-1}$ , giving an average of  $\Delta_D = 1364 \pm 300 \text{ cm}^{-1}$ . These values must be viewed as representing merely an order-of-magnitude determination.

If  $\Delta_D$  and  $\Delta_I$  are recognized as representing the same energy  $\Delta$ , then the mechanism can be understood as follows.<sup>25</sup> The observed effects can have a motional source. The apparent decrease of the peak height of spectrum I can be the result of a temperature variation of the relaxation time which, in this case, is directly related to the intensity  $I_p$ . The existence of an exponential law  $I_p \propto 1/T_1 \propto e^{-\Delta/kT}$  is suggested by Fig. 5. Similarly, spectrum III can originate from thermal averaging of spectrum I. As such, its growth, being inversely proportional to  $T_1$ , is expected to follow a similar exponential law,  $e^{\Delta/kT}$ , and to have the same activation energy  $\Delta$ .

The energy  $\Delta$  can have the following, intuitive, interpretation. The dependence of the electron potential on nuclear coordinates  $(\rho, \theta)$  can be described in  $Q_2$  and  $Q_3$  space by the familiar "Mexican hat" (see, for example, Fig. 6 of Ref. 1). In addition, the electronic energy is dependent on  $\theta$  through the so-called "warping term,"  $A_3 \rho^3 \cos 3\theta$ , originally introduced by Öpik and Pryce<sup>7</sup> and also discussed by O'Brien.<sup>8</sup> Öpik and Pryce estimate  $|A_3 \rho^3|$  to fall in the neighborhood of 700  $\text{cm}^{-1}$ . Our value for  $\Delta$ , which lies in the range 900–1600  $\text{cm}^{-1}$ , is reasonable for such an order-of-magnitude determination.

The following concluding remarks are in order.

(1) The linewidth of III depends on the nuclear spin quantum number  $m_I$ . This kind of dependence is well known<sup>26</sup>:

$$1/T_2 \approx \tau_c (\Delta g \beta H + K m_I)^2 / \hbar^2, \quad (9)$$

<sup>25</sup> Remarks in this and the following paragraph are based on comments made to the authors by Dr. F. S. Ham. We acknowledge this fact gratefully.

<sup>26</sup> G. E. Pake, *Paramagnetic Resonance* (Benjamin, New York, 1962), p. 110.

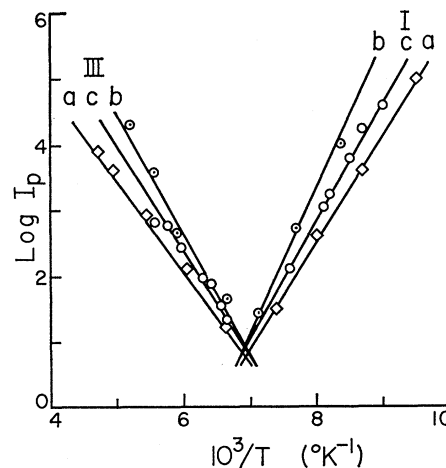


FIG. 5. Plots of logarithms of peak height  $I_p$  of spectra I and III versus  $1/T$ . (a)  $H \perp c$ , X band; (b)  $H \parallel c$ , X band; (c)  $H \parallel c$ , K band. The logarithms are to the base 10.

where, apart from standard symbols,  $\Delta g \beta H$  represents the difference between the two Zeeman levels involved in the relaxation process. According to Eq. (9) the lines are narrowest when  $\Delta g \beta H + K m_I$  is smallest. For  $H \parallel c$  the term in  $H$  is zero and the widths of all the lines of III should be [and are, according to Fig. 3(f)] of the same order of magnitude. Figure 2(b) shows that this fact holds also at a general orientation.

(2) III reaches a peak intensity at 230°K. The subsequent decrease may reflect the decrease in spin-lattice relaxation time, which would tend to broaden the resonances. A study of the spectrum at temperatures higher than 380°K was not possible since the lines were broadened too much.

#### ACKNOWLEDGMENTS

The authors would like to acknowledge the experimental assistance of Dr. L. Bonazzola and Dr. S. M. Quick.